Modelling Light Curves of Millisecond Period X-Ray Pulsars

C. Cadeau* and S.M. Morsink†
Theoretical Physics Institute, Department of Physics, University of Alberta, Edmonton, AB, T6G 2J1, Canada

Light curves of X-ray pulsars reveal characteristics of the underlying neutron star and emission region. To accurately interpret observations of millisecond period X-ray pulsars, one requires theoretical models of such light curves which fully account for general relativity and timing effects. This calculation is frequently done by employing one or more approximations, such as using an approximate spacetime, neglecting some time delay effects, or neglecting stellar oblateness. We are developing a new computer code to calculate these light curves which fully accounts for these effects; sample calculations are exhibited and presented alongside a similar calculation which employs commonly-used approximation techniques.

1. Introduction

Observations of pulsed light emitted from the surface of a neutron star have the potential to constrain the star's mass, radius and equation of state. By modelling the physics of the emission region (such as the emissivity, shape and size) and tracing the paths of photons travelling through the relativistic gravitational field of the spinning neutron star to the observer, it is possible to create model pulse shapes which can be compared to the observed pulse shapes, allowing fits to the star's macroscopic parameters to be made. The main problem in such a program is disentangling the effects arising from the neutron star's gravitational field and the effects coming from the assumptions about the spectrum and geometry of the emission region. A further complication arises if the neutron star is rotating rapidly, since the effects of rotation can significantly alter the geodesic paths travelled by the photons from the simple Schwarzschild geodesics.

A standard approximation scheme for ray-tracing near rotating neutron stars has been to treat the propagation of photons as though the gravitational field were static, so that the Schwarzschild metric and the formalism presented by Pechenick et al. [1983] can be used. The effects of rotation are brought in by introducing special relativistic Doppler boosts. The contribution of the light-crossing time is commonly neglected, which for millisecond period pulsars can be as long as about 80 μs, or 5% of the rotational period. Such an approximation scheme was recently used by Poutanen and Gierliński [2003] to fit the pulse profile of SAX J1808.4–3658 and to place constraints on the neutron star's value of M/R.

A different approximate approach has been to treat the gravitational field outside the neutron star as being approximately described by the Kerr metric with the Kerr parameter a fixed by the angular momentum of the underlying neutron star. This approach was applied to modelling the 314 Hz oscillations seen during thermonuclear bursts from the accreting millisecond pulsar XTE J1814–338 by Bhattacharyya et al. [2005] to obtain constraints on the compactness of the underlying neutron star; their approach included the contribution of the light-crossing time in the calculation of the model light curves, but employed an approximate spacetime metric, and approximated the shape of the star as spherical.

Cadeau et al. [2005] set out to determine what effect the use of such approximations would have on the stellar radius obtained by fitting theoretical light curves to observations. By considering a simple model where emission and observation of light take place in the equatorial plane, they demonstrated that this fitting procedure to obtain constraints on the neutron star's radius can result in errors on the radius of up to $\pm 10\%$ compared with a similar calculation where the spacetime is precisely calculated (i.e., not taken to be either Schwarzschild or Kerr) and all time of arrival (TOA) effects are accounted for.[1] The bulk of this error was due to neglecting the light-crossing time.

Continuing this programme, we have developed a new computer code to calculate light curves for these pulsars which allows for emission from arbitrary locations on the star's surface and observation at arbitrary inclinations. Our method uses an exact (numerical) calculation of the spacetime, and accounts for stellar oblateness and all TOA effects. Our code is also able to carry out analogous approximate calculations by selecting an approximate metric (i.e., Schwarzschild or Kerr), optionally approximating the

*Electronic address: ccadeau@phys.ualberta.ca
†Electronic address: morsink@phys.ualberta.ca

[1] To be clear, we are assuming that the effects due to the orbital period of the binary have been removed from the light curve; we are only concerned with those effects that arise due to special relativity (the "snapshot effect") and due to the varying distance light travels during a rotation of the neutron star (the "light-crossing time").

star as a sphere (as opposed to an oblate spheroid), or disregarding some or all TOA effects. We are presenting an overview of the method and some preliminary light curve calculations with all effects included. In Section 3.4 we show two exact calculations alongside approximate versions where the spacetime is approximated as Schwarzschild, oblateness is not accounted for, and the TOA effects are not fully accounted for.

2. Formulation of Problem

To compute the pulse shape we wish to know the flux F at each instant, where

$$F = \int_{(1+z)\nu_{o_{\rm low}}}^{(1+z)\nu_{o_{\rm high}}} {\rm d}\nu_{\rm e} \int {\rm d}\Omega\, I_{\nu_e}(\alpha_e)/(1+z)^4,$$

and the integral depends on the observed frequencies of light, which range from $\nu_{o_{\rm low}}$ to $\nu_{o_{\rm high}}$, the intensity I of the emitted light as a function of emitted frequency ν_e and zenith angle α of the emitted beam, the redshift of the light z, and the element of solid angle in the observer's sky ${\rm d}\Omega$.

To carry out this calculation, one needs to decide on the description of the gravitational field of the star; the manner in which to handle relative TOAs of photons; the inclination of the star with respect to the observer; the location of emitting region; and the emission spectrum and anisotropy (if any) of the emitting region. With all of this information, we can compute the light curve for the model pulsar.

2.1. Gravitational field

Typically, the Schwarzschild or Kerr metrics are used as approximations to the precise neutron star metric by matching parameters (M/R, J) of the underlying neutron star. Using the computer code RNS [Stergioulas and Friedman 1995], it is possible to precisely compute the stellar structure and the components of the general stationary axisymmetric metric,

$$\begin{aligned} {\rm d}s^2 &= -e^{\gamma+\rho}\,{\rm d}t^2 + e^{\gamma-\rho} r^2 \sin^2\theta ({\rm d}\phi - \omega\,{\rm d}t)^2 \\ &\quad + e^{2\alpha}({\rm d}r^2 + r^2\,{\rm d}\theta^2), \end{aligned}$$

where γ, ρ, ω, and α are all functions of r and θ only, by assuming that the matter comprising the star is a rigidly-rotating perfect fluid. The code requires the mass and angular velocity of the star and the equation of state (EOS) of the fluid, and outputs the metric components and their derivatives, and details of the neutron star's structure. If one desires an approximate metric, the metric components are analytically determined given M, R, and J. With a choice of metric in hand, we integrate the geodesic equations which determine the path light follows from the star to the observer using an adaptive step size Runge-Kutta routine.

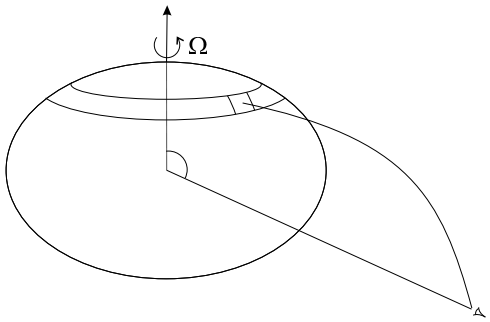

Figure 1: To carry out the calculation, a small quadrilateral is evolved around one rotational period, at each step recording the emitted flux and arrival time.

2.2. Time of arrival (TOA)

Time of arrival effects can be, and commonly are, thought of only in the sense of the special relativistic "snapshot" effect [Terrell 1959], where the apparent angular size of the emission region is magnified when it is moving away from the observer, owing to the image in the detector being formed by photons emitted at different times from different parts of the star. The flux is integrated as a function of rotational phase, with the solid angle transformation factor put in by hand.

For rapid rotation, the contribution of the light-crossing time begins to be important, as the photons emitted from the far side of the star can take measurably longer to arrive than those from the near side. By calculating the light travel times during the integration of the geodesic equations, the flux due to an infinitesimal emission region can be correctly binned *as a function of arrival time*, not rotational phase. No additional correction factor is required when this is done. Our actual procedure to carry out the calculation is to evolve a small quadrilateral around one period as depicted in Figure 1, at each step calculating the emitted flux and the arrival time of the flux, and we output the flux as a function of arrival time. In this way, the flux from extended regions can be calculated by properly adding the fluxes from different latitudes and phase offsets.

3. Example calculations

Our code allows for the modelling of various emission spectra and anisotropy, but for the purposes here we are restricting the light curves that follow to bolometric flux emitted isotropically from an infinitesimal region at the surface. In Sections 3.1, 3.2, and 3.3, we use a full calculation where the exact spacetime is used and all TOA effects are included. In Section 3.4, we compare some calculations to their approximate analogues.

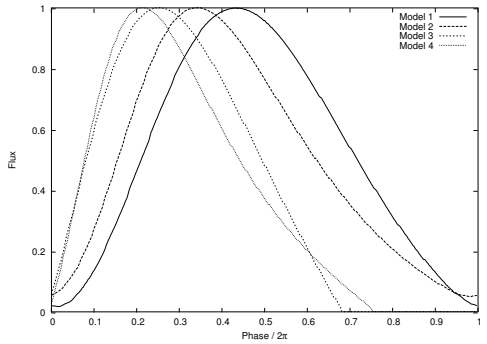

Figure 2: Bolometric light curves for the four models of Table I. Light is emitted at $\theta = 45°$ and observed in the equatorial plane in this example.

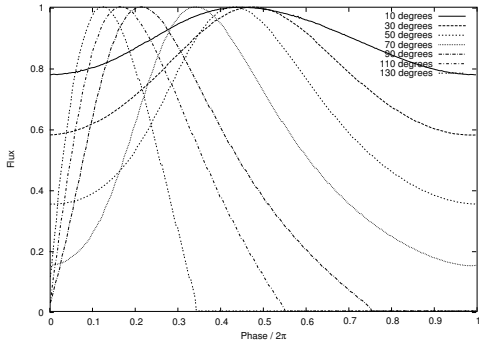

Figure 3: Bolometric light curves for Model 4, where the observer is located at different inclinations θ as measured from the rotation axis, and light is emitted from $\theta = 45°$.

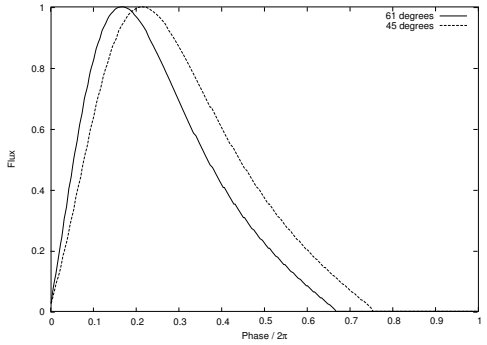

Figure 4: Bolometric light curves for Model 4, where the observer is located in the equatorial plane, and the emission region is at either $\theta = 45°$ or $\theta = 61°$ as measured from the rotation axis.

3.1. Choice of model

In this section, we consider an emission region located at $\theta = 45°$ and the observer located in the equatorial plane at $\theta = 90°$ for each of the four models listed in Table I. EOS A is relatively soft, and so Models 1 and 2 are relatively compact. EOS L is stiffer, and so Models 3 and 4 are relatively large. Model 4 is spinning quite near its breakup speed.

From Figure 2, one can see that more compact stars have light visible for a longer fraction of their period due to light bending. Also, increased rotation speed has the effect of making the rise time of the light curve shorter compared with the fall time owing to the larger blueshift/redshift along the line of sight. Finally, the effect due to light-crossing time is exaggerated for the 600 Hz cases because one light-crossing time represents a larger fraction of the rotational period for the faster stars.

3.2. Effect of observer inclination

Figure 3 shows several light curves computed using Model 4 for an emission region located at $\theta = 45°$, but for observers with different inclinations as measured from the rotation axis. The computed light curves have been phase-shifted to align the rise for each observer. As expected, observers closer to the rotation axis in the hemisphere of emission see less modulation in the signal than the observers with large inclinations.

3.3. Effect of emitting region location

Figure 4 shows light curves computed using Model 4 for an observer located in the equatorial plane at $\theta = 90°$, but for emission from $\theta = 45°$ and $\theta = 61°$. The computed light curves have been phase-shifted to align the rise for each emitting region. Note that the 61° light curve peaks faster than the 45° light curve; this is due to the higher velocities at the surface, and therefore larger Doppler effects, as one moves towards the equator.

3.4. Effect of Schwarzschild approximation

In this section, we are considering emission from $\theta = 45°$ seen by an observer in the equatorial plane. Figure 5 compares two calculations for Model 1: a calculation using the exact spacetime and accounting for TOA effects ("Exact"), and a calculation using the Schwarzschild metric for a spherical star with the same M/R as Model 1 and accounting for only the "snapshot" effect, but not the light-crossing time ("Schw."). Figure 6 is a similar plot for Model 4. One can see that an effect of including the light-crossing time is that the exact calculations appear to have visible light for a longer fraction of the period; notably, in the case of Figure 5, the light is always visible for the exact calculation but not using the Schwarzschild version. It is unclear whether this is an effect of replacing the oblate star with a spherical one in the approximation, or an effect solely due to light-crossing time; this is an issue we are pursuing. Also, the departure from

Table I Neutron star models with mass $M = 1.4M_\odot$

Model	EOS	$\Omega_B/2\pi^a$	$\Omega_\star/2\pi^b$ (Hz)	R^c (km)	$cJ/(GM^2)^d$	$GM/(c^2R)$	v/c^e	$\omega_{eq}/2\pi^f$ (Hz)
1	A	1387	300	9.62	0.109	0.21	0.08	50.2
2			600	9.78	0.223	0.21	0.16	98.3
3	L	742	300	15.11	0.234	0.14	0.11	27.9
4			600	16.38	0.508	0.13	0.24	48.9

[a]The break-up spin frequency for a star with the given mass and EOS.
[b]The spin frequency of the model.
[c]The equatorial Schwarzschild radius.
[d]The angular momentum of the model
[e]The speed of the neutron star at the equator measured by a static observer at the surface. Velocities are calculated with the full metric.
[f]The frame-dragging term at the equator; this is the angular velocity of a zero angular momentum particle at the equator.

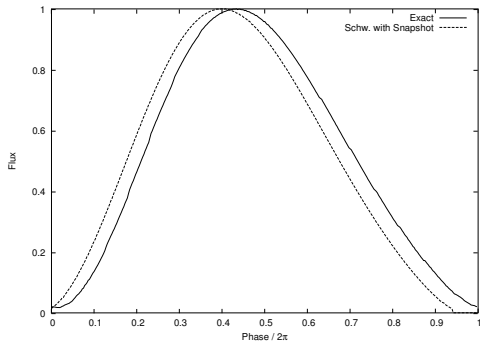

Figure 5: Bolometric light curves for Model 1, comparing a full calculation using the exact metric and all TOA effects with a calculation using the Schwarzschild metric with the same M/R and incorporating only the "snapshot" effect.

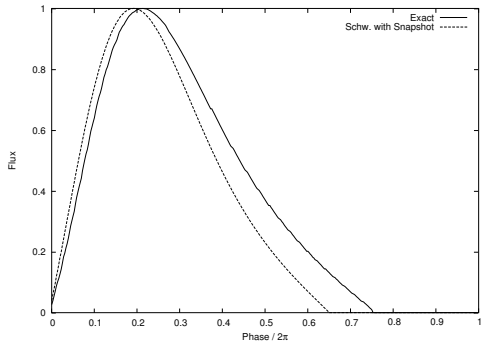

Figure 6: Calculations similar to Figure 5, but for Model 4.

the approximation appears more pronounced for the faster and larger star in Figure 6, which can be understood as an effect of its longer crossing time and a shorter rotational period.

4. Conclusion

We have made progress implementing a new code to calculate light curves of millisecond period pulsars which uses a precise prescription of the spacetime and stellar structure and properly accounts for all TOA effects. Our current work is focused on quantifying the effect of using different approximate techniques in the calculation of theoretical light curves on the resulting interpretation of X-ray observations from accreting millisecond period X-ray pulsars. A description of our code and discussion of implications for data analysis is forthcoming.

Acknowledgments

CC is grateful for financial assistance from the conference organisers which made it possible to attend the XXII Texas Symposium on Relativistic Astrophysics.

This work is supported by a grant from the Natural Sciences and Engineering Research Council of Canada (NSERC) held by SMM.

The authors wish to thank Denis A. Leahy for valuable conversations, and the Theoretical Physics Institute at the University of Alberta for hosting visits of DL to Edmonton.

Numerical solutions for neutron star spacetimes were calculated using the RNS software by Nikolaos Stergioulas. This software is available at `http://www.gravity.phys.uwm.edu/rns`.

References

K. Pechenick, C. Ftaclas, and J. Cohen, Astrophys. J. **274**, 846 (1983).

J. Poutanen and M. Gierliński, Mon. Not. R. Astron. Soc. **343**, 1301 (2003).

S. Bhattacharyya, T. Strohmayer, M. Miller, and C. Markwardt, Astrophys. J. **619**, 483 (2005).
C. Cadeau, D. Leahy, and S. Morsink, Astrophys. J. **618**, 451 (2005).
N. Stergioulas and J. Friedman, Astrophys. J. **444**, 306 (1995).
J. Terrell, Phys. Rev. **116**, 1041 (1959).